

---

# Causal Discovery under Latent Class Confounding

---

**Bijan Mazaheri\***

Eric and Wendy Schmidt Center  
Broad Institute of MIT and Harvard  
Cambridge, MA 02142  
bmazaher@broadinstitute.org

**Spencer Gordon**

Department of Computer Science  
University of Liverpool  
Liverpool, UK  
slgordon@liverpool.ac.uk

**Yuval Rabani**

Department of Computer Science  
Hebrew Institute of Jerusalem  
Jerusalem, Israel  
yrabani@cs.huji.ac.il

**Leonard Schulman**

Department of Computer Science  
California Institute of Technology  
Pasadena, CA  
schulman@caltech.edu

## Abstract

An acyclic causal structure can be described using a directed acyclic graph (DAG) with arrows indicating causation. The task of learning this structure from data is known as “causal discovery.” Diverse populations or changing environments can sometimes give rise to heterogeneous data. This heterogeneity can be thought of as a mixture model with multiple “sources,” each exerting their own distinct signature on the observed variables. From this perspective, the source is a latent common cause for every observed variable. While some methods for causal discovery are able to work around unobserved confounding in special cases, the only known ways to deal with a global confounder (such as a latent class) involve parametric assumptions. Focusing on discrete observables, we demonstrate that globally confounded causal structures can still be identifiable without parametric assumptions, so long as the number of latent classes remains small relative to the size and sparsity of the underlying DAG.

## 1 Introduction

**Structural Causal Models** Many modern approaches to studying causal systems use structural causal models (SCMs) to graphically model causal relationships in a directed acyclic graph (DAG) [Pearl, 2009, Peters et al., 2017]. In an SCM,  $A \rightarrow B$  indicates “ $A$  has a direct effect on  $B$ .” These graphical models provide a systematic way of determining covariate adjustments to identify the effects of interventions.

“Causal discovery” is the task of recovering a causal DAG from data. The simplest algorithms for causal discovery make use of a correspondence between the conditional independence of the observed variables and graphical properties of the underlying SCM. These “d-separation rules”<sup>2</sup> give graphical criteria for independence and dependence under an assumption known as faithfulness. For example,  $A \not\perp B$  and  $A \perp\!\!\!\perp C \mid B$  is sufficient to conclude that there is no arrow between  $A$  and  $C$ . We say that  $B$  is a “separating set” for  $A, C$  and conclude that there are three possible structures:  $A \rightarrow B \rightarrow C$ ,  $A \leftarrow B \leftarrow C$  or  $A \leftarrow B \rightarrow C$ . Together, we say these three structures form a “Markov equivalence

---

\*Work primarily done during Ph.D. at Caltech. <http://bijanmazaheri.com>

<sup>2</sup>See Pearl [2009] for a review of d-separation or Appendix A for a summary of important results used in this manuscript.

class,” which can be described using a CPDAG, i.e. the undirected skeleton of the true graph and partial orientation of the edges.

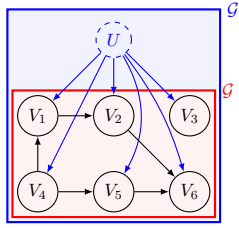


Figure 1: The goal is to learn the graph structure  $\mathcal{G}$  without observing  $U$ .

**Problem Statement** Suppose we augment a DAG  $\mathcal{G} = (\mathbf{V}, \mathbf{E})$  with an unobserved  $U$  that has  $k$  “latent classes,” each of which leaves a distinctive signal on all the observed variables  $\mathbf{V}$ . The result is a mixture-model whose DAG,  $\mathcal{G}' = (\mathbf{V} \cup \{U\}, \mathbf{E}')$  includes additional arrows from the “universal confounder” to every  $V \in \mathbf{V}$ . See Figure 1 for an example. We will refer to  $\mathcal{G}$  as the observed sub-graph and we will use  $\Delta := \max_{V \in \mathbf{V}} \deg^{\mathcal{G}}(V)$  to denote its maximum (in plus out) degree.

The goal is to uncover the observed sub-graph’s structure  $\mathcal{G}$  up to a Markov equivalence class (i.e. a CPDAG) using statistics gained from the “observed probability distribution,” i.e.  $\Pr(\mathbf{V})$  marginalized over  $U$ . Notice that  $U$  confounds all pairs of variables in  $\mathbf{V}$ , which requires it to be in *every* separating set. This means that the correspondence between conditional independence and d-separation is no longer adequate to make any structural deductions about the graph.

**Assumptions** We will assume (1) that the distribution is faithful<sup>3</sup> with respect to  $\mathcal{G}'$ , and (2) that  $U$  is discrete with a known number of latent classes  $k$ .  $k$  represents the “complexity” of unobserved confounding, as more latent classes are capable of exerting “more complex” signals. Since our deductions rely upon each value of  $U$  having distinctive effects upon the observables, the most difficult case of the problem is Bernoulli observable variables. Compositions of such variables are adequate to express any finite-range variables. Hence we focus entirely upon the case of Bernoulli observables.

**Causal discovery with unobserved confounding** The PC algorithm was the first causal discovery algorithm to make use of conditional independence, outlined in [Spirtes et al., 2000a]. Many causal discovery algorithms have been developed since, summarized in Squires and Uhler [2023]. A number of these algorithms address the presence of latent confounding using one of two assumptions that “limit”  $U$ , neither of which apply to our setting.

The first type of assumption involves limiting the *degree* of latent confounding. For example, the FCI algorithm can detect the presence of unobserved confounders that act on *only two* observed variables [Spirtes et al., 1993, Spirtes, 2001]. Richardson and Spirtes [2002]’s seminal work introduced ancestral graphs for the general study of this setting. Unfortunately, this assumption cannot be applied to a global or “pervasive” confounder.

The second type of assumption is on the parametric nature of the structural equations. For example, Frot et al. [2019] was able to show superior performance in settings with large-degree confounders with linear relationships and additive sub-Gaussian or elliptical noise. Other settings include linear structural equations with non-Gaussian additive noise [Cai et al., 2023] and non-linear structural equations within a finite-dimensional Hilbert space [Agrawal et al., 2023]. These approaches are incapable of addressing *discrete*  $U, \mathbf{V}$ , which have no restriction on their noise or structural equations.

## 1.1 Motivation

**Heterogeneous Data** Whenever data spans multiple populations, environments, or laboratories, the relationships within are subject to “global” or “pervasive” confounding [Gordon et al., 2023b]. In these settings, true causal relationships become entangled with spurious indicators of population (or

<sup>3</sup>The precise assumption is a slight extension of faithfulness to the mixture setting, discussed later.

lab source, etc.) membership. While these data-sources are sometimes observed, naive adjustments for global confounding require conditioning on the data-source, which limits the power of a joined dataset. Recovering a smaller subset of latent “classes” of data-sources is therefore essential to the problem of data-fusion [Castanedo, 2013]. This task involves learning a mixture model, ie. uncovering “mixture weights”  $\Pr(U)$  and “source distributions”  $\Pr(\mathbf{V} | U)$ .

**Mixture Models** Most work on mixture models deals with parametric distributions. The simplest example is a Gaussian mixture, which relies on the parametric assumption of Gaussianity to recover clusters of points. Without this assumption, there is no way to tell the difference between a mixture of two mono-modal (one hump) distributions versus a single bi-modal (two humps) distribution.

Discrete data poses an interesting challenge because categorical distributions are non-parametric. Notice that the statistics gathered from a single unbiased coin are exactly the same as those gathered from two biased coins with the same average bias (e.g.  $1/3$  and  $2/3$ ), so long as we are limited to a *single sample* from each choice of coin. Almost all of the research in this setting leverages an assumption of mutually independent observed variables within the source distributions [Cryan et al., 2001, Freund and Mansour, 1999, Chaudhuri and Rao, 2008, Feldman et al., 2008, Rabani et al., 2014, Chen and Moitra, 2019, Gordon et al., 2021, 2023a] (see also the earlier seminal work of Kearns et al. [1994]). We call this the  $k$ -MixProd problem, whose identifiability is discussed in more detail in Appendix B.

$k$ -MixProd amounts to a graphical assumption, i.e. that the causal model within each source is an empty graph. Early work by Anandkumar et al. [2012] and Gordon et al. [2023b] broadened this class of independence assumptions for mixture identifiability, exploring Markov random fields and Bayesian networks respectively.

A key assumption of [Gordon et al., 2023b] and  $k$ -MixProd is that the Bayesian DAG structure within each mixture component is *known*. To date there is no result showing if and when the within-source DAG structure can be identified from the observed data of a mixture model. If we are capable of recovering graphical structure in this setting, then we can use that structure to recover the mixture without ever making parametric or structural assumptions.

**Other Related Work** Other work has investigated a different setting in which *different DAG structures* are mixed [Saeed et al., 2020]. This work relies on the preservation of some local conditional independence properties to learn a “union graph.”

## 1.2 Main Result

This paper will give the first proof of the identifiability of causal structures within the discrete mixture setting by developing the first known algorithm for this problem.

**Theorem 1.** Consider  $\mathcal{G} = (\mathbf{V}, \mathbf{E})$  with  $\Omega(\log(k)\Delta^3)$  vertices, mixture source  $U \in \{1, \dots, k\}$  and degree bound  $\Delta$ .  $\mathcal{G}$  is generically<sup>4</sup> identifiable up to its Markov equivalence class.

Using an oracle that can solve  $k$ -MixProd in time  $\tau$  and an oracle that can solve for non-negative rank in time  $\rho$  we give an algorithm that runs in time  $|\mathbf{V}|^{\mathcal{O}(\Delta^2 \log(k))} \rho + \mathcal{O}(k|\mathbf{E}|2^{\Delta^2})\tau$ . See Appendix C for further discussion on the runtime of  $\rho$  and  $\tau$ .

Our algorithm will build on two key ideas. The first of these ideas is that the rank of a matrix formed by the joint probabilities of two variables contains information about the graphical structure on those variables under latent class confounding. We observe that the joint probability distribution of two independent variables of cardinality  $\ell$  forms an  $\ell \times \ell$  matrix that can be written as a rank 1 outer-product. Hence, marginalizing over a  $k$ -mixture gives us a linear combination of these rank 1 matrices, which will generically be rank  $k$ .

Of course, finite data only affords a stochastic perturbation of the true matrix of joint probabilities. A naive approach to testing the rank of the underlying joint probability distribution involves thresholding singular values as in Anandkumar et al. [2012]. Such an approach is unstable, with many practical difficulties associated with selecting the correct threshold. Instead, we modify a statistical test based on Ratsimalahelo [2001] to obtain a hypothesis test for the rank of an estimated joint probability

<sup>4</sup>with Lebesgue measure 1 in the space of observed moments.

matrix. We demonstrate the superiority of this approach and note that this test may be of fundamental use in other mixture settings.

The idea of using matrix rank is limited by the cardinality of our variables – the joint probability distribution of two binary observables forms a  $2 \times 2$  matrix whose rank is no larger than 2. This problem leads to the second idea: We can “coarsen” variables by joining sets of variables. These “super variables” take on values in the Cartesian product of their components’ alphabets. For example, three Bernoulli variables can be combined into a single variable of cardinality 8. This paper develops the notion of testing rank on these coarsened variables for causal discovery.

### 1.3 Outline of Algorithm

The PC-algorithm works in two phases. The first phase begins with a complete graph (i.e. all possible edges) and uses conditional independence tests to find non-adjacencies and “separating sets” that d-separate them. When a non-adjacency is found, the corresponding edge is removed and its separating set is stored. The second phase uses the separating sets from the first phase to orient immoralities (as well as further propagation of edge orientation via Meek rules).

Our algorithm will mirror the PC Algorithm, but will split the first phase into two parts, yielding three total phases. Phase I will again begin with a complete graph and remove edges between variables when we find evidence of non-adjacency (this time using rank tests).

Phase I will only test independence on groupings of variables, so its termination will not guarantee that we have discovered all possible non-adjacencies. Instead, a provably small subset of the graph will have *false positive* edges. In Phase II, we will make use of the structure we have uncovered so far to induce instances of  $k$ -MixProd within conditional probability distributions. A  $k$ -MixProd solver will then identify the joint probability distribution between subsets of  $V$  and the latent class  $U$ . Access to this joint probability distribution enables a search for separating sets that include  $U$ , meaning that the rest of the structure can be resolved using traditional conditional independence tests (following the standard steps of the PC algorithm).

Phase III mirrors the last phase of the PC algorithm: identifying immoralities using non-adjacencies and separating sets, then propagating orientations according to Meek rules. This phase is no different from the PC algorithm, so we will not discuss this phase in detail.

### 1.4 Notation

We will use the capital Latin alphabet to denote random variables, which are vertices on our DAG. When referring to sets of these variables, we will use bolded font, e.g.  $\mathbf{X} = \{X_1, X_2, \dots\}$ . To refer to components of a graph, we will use the following operators:  $\mathbf{PA}(V)$ ,  $\mathbf{CH}(V)$  will refer to the parents and children of  $V$ .  $\mathbf{AN}(V)$ ,  $\mathbf{DE}(V)$  will refer to the ancestors and descendants of  $V$ .  $\mathbf{AN}(V) \cup \{V\}$  and  $\mathbf{DE}(V) \cup \{V\}$  are denoted using  $\mathbf{AN}^+(V)$ ,  $\mathbf{DE}^+(V)$  respectively.  $\mathbf{MB}(V) = \mathbf{PA}(V) \cup \mathbf{CH}(V) \cup \mathbf{PA}(\mathbf{CH}(V))$  will refer to the Markov boundary (i.e. the unique minimal Markov blanket) of  $V$  [Pearl, 2009].  $\mathbf{NB}_\ell(V)$  refers to the distance  $\ell$  neighborhood of  $V$ .

As these operators act on graphs, they can specify the graph structure being used in the superscript, e.g.  $\mathbf{PA}^{\mathcal{G}}(V)$ . Unless otherwise specified, operators should be assumed to apply to the observed subgraph  $\mathcal{G}$  and not  $\mathcal{G}'$ , i.e.  $U \notin \mathbf{PA}^{\mathcal{G}}(V)$ . We will also occasionally write tuples to indicate the intersection of the sets for two vertices, e.g.  $\mathbf{CH}(V, W) = \mathbf{CH}(V) \cap \mathbf{CH}(W)$ . Finally, these operators can also act on sets to indicate the union of the operation, e.g.

$$\mathbf{PA}(\mathbf{X}) = \bigcup_{X \in \mathbf{X}} \mathbf{PA}(X) \setminus X. \quad (1)$$

We make use of lowercase letters to denote assignments, for example  $x$  will denote the assignment  $X = x$ . This can also be applied to operators, e.g.  $\mathbf{mb}(V)$  denotes an assignment to  $\mathbf{MB}(V)$ . Assignments for these operators can also be obtained from a larger set of assignments using a subscript, e.g.  $\mathbf{mb}_c(V)$  obtains assignments for  $\mathbf{MB}(V) \subseteq C$  from the assignments of  $c$  to  $C$ .  $\text{rk}_+(\mathcal{M})$  will denote the nonnegative rank of matrix  $\mathcal{M}$ .

## 2 Rank Tests

This section will develop “rank tests” which will serve as a replacement for conditional independence tests as a test for d-separation or d-connectedness.

### 2.1 Checking for $k$ -Mixture Independence

To determine non-adjacency, we will take advantage of a signature  $U$  leaves on the marginal probability distributions of variables which are independent conditional on  $U$ . First, we interpret the marginal probability distribution as a matrix.

**Definition 1.** Given two discrete variables  $X, Y \in \mathcal{V}$  each with  $|X| = |Y| = m$ , define the “probability matrix”  $\mathcal{M}[X, Y] \in [0, 1]^{m \times m}$  to be

$$\mathcal{M}[X, Y]_{x,y} := \Pr(x, y), \quad (2)$$

where  $x, y$  both range from  $1, \dots, m$ . Similarly, for  $\mathcal{C} \subseteq \mathcal{V}$ , define

$$\mathcal{M}[X, Y | \mathcal{C}]_{x,y} := \Pr(x, y | \mathcal{C}). \quad (3)$$

We now notice that we can decompose the probability matrix into a linear combination of conditional probability matrices for each source, for which Lemma 1 gives an upper bound on rank.

**Lemma 1.** *Given a mixture of Bayesian network distributions that are Markovian in  $\mathcal{G}$ , if  $X \perp\!\!\!\perp_d^{\mathcal{G}} Y | \mathcal{C}$ , then for all  $\mathcal{C}$ ,  $\text{rk}_+(\mathcal{M}[X, Y | \mathcal{C}]) \leq k$ .*

*Proof.* We can decompose  $\mathcal{M}[X, Y | \mathcal{C}]$  as follows,

$$\mathcal{M}[X, Y | \mathcal{C}] = \sum_u \Pr(u) \mathcal{M}[X, Y | \mathcal{C}, u]. \quad (4)$$

$X \perp\!\!\!\perp Y | \mathcal{C}, U$ , so  $\mathcal{M}[X, Y | \mathcal{C}, u]$  can be written as the outer product of two vectors describing the probabilities of each variable. Therefore, we conclude that  $\text{rk}_+(\mathcal{M}[X, Y | \mathcal{C}, u]) = 1$ . If  $U \in [k]$ , then  $\text{rk}_+(\mathcal{M}[X, Y | \mathcal{C}]) \leq k$ .  $\square$

Having shown that d-separation in  $\mathcal{G}$  upper bounds the rank of probability matrices, we now seek a lower bound on the rank in the case of d-connectedness. This will require a “faithfulness-like” assumption that the dependence exerts some noticeable effect between the two variables. Lemma 2 shows that such a condition holds generically.

**Lemma 2.** *Given a mixture of Bayesian network distributions, each of which is faithful to  $\mathcal{G}$ . If  $X \not\perp\!\!\!\perp_d^{\mathcal{G}} Y | \mathcal{C}$  and  $|X| = n, |Y| = m$  with  $n, m > k$ , then for all  $\mathcal{C}$ ,  $\text{rk}_+(\mathcal{M}[X, Y | \mathcal{C}]) > k$  with Lebesgue measure 1.*

The proof of Lemma 2 (see Appendix F) involves applying faithfulness to each component of the decomposition in Equation 4. Lemma 1 and Lemma 2 provide a generically necessary and sufficient condition for detecting  $V_i \perp\!\!\!\perp_d^{\mathcal{G}} V_j$ .

**Lemma 3 (Rank Test).** *For  $V_i, V_j$  with cardinality  $> k$ ,  $V_i \perp\!\!\!\perp_d^{\mathcal{G}} V_j | \mathcal{C}$  if and only if (generically)  $\text{rk}_+(\mathcal{M}[V_i, V_j | \mathcal{C}]) \leq k$ .*

### 2.2 Hypothesis test for rank

We can build a hypothesis test for the null-hypothesis that  $\mathcal{A} := \mathcal{M}[V_i, V_j | \mathcal{C}]$  is has rank  $\leq k$ . First, decompose  $\mathcal{A}$  according to the SVD  $\mathcal{A} = \mathcal{V}\mathcal{D}\mathcal{U}^\top$ . If  $\mathcal{A} \in \mathbb{R}^{m \times m}$  is rank  $k$ , we will have  $\mathcal{U}, \mathcal{V} \in \mathbb{R}^{k \times m}$ . When this decomposition is done on the empirical matrix,  $\hat{\mathcal{A}}$ , we define  $\mathcal{U}_2$  and  $\mathcal{V}_2$  to be the  $k + 1$ th to  $m$ th “extra” rows of  $\mathcal{U}$  and  $\mathcal{V}$  respectively, and  $\mathcal{L}$  to be the diagonal matrix with the  $k + 1$ th through  $m$ th singular values. Vectorize  $\mathcal{L}$  to  $\hat{\mathcal{L}}$  by stacking the columns of  $\mathcal{L}$ . Let  $\Sigma$  be the covariance matrix of the entries of  $\mathcal{A}$  with similar stacking, i.e.

$$\Sigma_{i+jm, i'+j'm} := \text{Cov}(\mathcal{A}_{ij}, \mathcal{A}_{i'j'}). \quad (5)$$

Now, with  $\hat{\Sigma}^\dagger$  indicating the Moore-Penrose pseudoinverse of  $\hat{\Sigma}$  and  $\otimes$  indicating the Kronecker product, define

$$\hat{\mathcal{Q}}^\dagger := (\mathbf{v}_2^\top \otimes \mathbf{u}_2^\top) \hat{\Sigma}^\dagger (\mathbf{v}_2 \otimes \mathbf{u}_2). \quad (6)$$

According to Ratsimalahelo [2001], if  $f$  is the rank of  $\Sigma$ , then  $N\hat{l}^\top \hat{\mathcal{Q}}^\dagger \hat{l}$  converges to  $\chi_f^2$  under  $N$  samples.

We can use this test statistic with a simplified  $\hat{\Sigma}$  by noting that  $\hat{\mathcal{A}}$  for a single data-point is 0 for all but a single entry, which is 1. This means that the variance of an entry is given by the variance of a Bernoulli random variable and the covariance is given by the expanding into three cases: both are 0, the first entry is 1, the second entry is 1. This simplifies to

$$\text{Cov}(\mathcal{A}_{ij}, \mathcal{A}_{i'j'}) = \begin{cases} \mathcal{A}_{ij}(1 - \mathcal{A}_{ij}) & \text{if } i = i', j = j' \\ -\mathcal{A}_{ij}\mathcal{A}_{i'j'} & \text{otherwise.} \end{cases} \quad (7)$$

Using this estimate for  $\hat{\Sigma}$  gives us a hypothesis test that is specifically designed to implement the rank test from this section. This approach is tested and compared to thresholding the  $k + 1$ th singular value in Section 4.

### 3 Algorithm

We will now outline the first two phases of our algorithm, leaving out the final phase of orienting edges with respect to Meek’s rules. The first phase involves coarsening sets of variables and applying rank tests. We then analyze the output of the first phase  $\mathcal{G}_1$  which has removed *most but not all* of the missing edges. We define FP edges as these “leftovers” and show that they are contained within a subset of bounded size. This fact allows us to resolve all of the non-adjacencies in  $\mathcal{G}$  by setting up instances of  $k$ -MixProd in Phase II.

#### 3.1 Phase I: Coarsened Rank Tests

Lemma 3 allows for a simple generalization of classical structure-learning algorithms (such as the PC algorithm) provided that our probability matrix  $\mathcal{M}[X, Y]$  is large enough. Unfortunately, categorical variables ranging over smaller alphabets (such as the binary alphabets addressed by this paper) do not contain sufficient information to detect non-adjacency in cases of larger  $k$ . We resolve this problem by coarsening sets of small-alphabet (binary) variables into supervariables of larger cardinality.

**Definition 2.** Consider DAG  $\mathcal{G} = (\mathbf{V}, \mathbf{E})$ ,  $V_i, V_j \in \mathbf{V}$ , and sets  $\mathcal{S}_i, \mathcal{S}_j \subseteq \mathbf{V} \setminus \{V_i, V_j\}$ . We call the ordered pair  $(\mathcal{S}_i^+, \mathcal{S}_j^+) = (\mathcal{S}_i \cup \{V_i\}, \mathcal{S}_j \cup \{V_j\})$  an **independence preserving augmentation (IPA)** of  $(V_i, V_j)$  if, for some **IPA conditioning set**  $\mathcal{C} \subset \mathbf{V}$ ,

$$\mathcal{S}_i^+ \perp\!\!\!\perp_d^{\mathcal{G}} \mathcal{S}_j^+ \mid \mathcal{C}.$$

The creation of supervariables allows us to use conditional rank tests in the place of conditional independence tests. This leads to a modified version of the PC algorithm that searches over pairs of supervariable coarsenings instead of pairs of vertices, given in Algorithm 1.

**Lemma 4.** *Algorithm 1 utilizes  $|\mathbf{V}|^{\mathcal{O}(\Delta^2 \log(k))}$  non-negative rank tests.*

*Proof.* Lemma 11 tells us that the maximum size of a separating set, is  $\alpha := (\lceil \lg(k) \rceil + 1)\Delta^2$ , so we need to check  $\binom{|\mathbf{V}|}{\alpha} + \binom{|\mathbf{V}|}{\alpha-1} + \dots + \binom{|\mathbf{V}|}{1}$  possible separating sets, which is  $|\mathbf{V}|^{\mathcal{O}(\Delta^2 \log(k))}$ . We must iterate over all possible supervariables for each separating sets, which is upper bounded by  $\binom{|\mathbf{V}|}{2(\lceil \lg(k) \rceil + 1)}$ , which is  $|\mathbf{V}|^{\mathcal{O}(\log(k))}$ .  $\square$

##### 3.1.1 FP Edges

Phase I of our algorithm removes an edge between two non-adjacent variables through a rank test so long as there exists an IPA for the non-adjacency. Not all non-adjacencies will contain an IPA, so the adjacency graph  $\mathcal{G}_1$  contains a *superset* of the true adjacencies.

**Definition 3.**  $E_1 \setminus E$  are **false positive (FP)** edges.

### Algorithm 1: Phase I

**Input:** The marginal probability distribution  $\Pr(\mathbf{V})$ , marginalized over  $U$ .

**Output:** An undirected graph  $\mathcal{G}_1 = (\mathbf{V}, \mathbf{E}_1)$  and a separating set  $\mathcal{C}_{i,j}$  for each detected non-adjacency.

Begin with a complete undirected graph  $\mathcal{G}_1 = (\mathbf{V}, \mathbf{V} \times \mathbf{V})$  and  $d_{\max} \leftarrow |\mathbf{V}| - 1$ .

```

for  $\ell = 0$  to  $\ell = d_{\max}$  do
  for  $\mathcal{C} \subset \mathbf{V}$  and  $|\mathcal{C}| = \ell$  do
    for  $\mathcal{S}, \mathcal{S}' \subseteq \mathbf{V} \setminus \mathcal{C}$ , with  $|\mathcal{S}| = |\mathcal{S}'| = \lceil \lg(k) \rceil + 1$  do
      if arbitrary assignment  $c$  has  $\text{rk}_+(\mathcal{M}[\mathcal{S}, \mathcal{S}' | c]) \leq k$  then
        Remove all edges between  $\mathcal{S}$  and  $\mathcal{S}'$  in  $\mathcal{G}_1$ .
         $\mathcal{C}_{i,j} \leftarrow \mathcal{C}$  for each  $V_i \in \mathcal{S}, V_j \in \mathcal{S}'$ 
        Update  $\Delta$  to the maximum degree of  $\mathcal{G}_1$ .
      end
    end
  end
end

```

To see why FP edges exist, we will introduce the notion of immoral descendants.

**Definition 4** (Immoral Descendants). For non-adjacent  $V_i, V_j$  the **immoral descendants** of  $V_i$  and  $V_j$  are their co-children (often called immoralities [Pearl, 2009]) and those children's descendants.

$$\text{IMD}(V_i, V_j) := \text{CH}(V_i, V_j) \cup \text{DE}(\text{CH}(V_i, V_j)) \quad (8)$$

**Observation 1.** Any set  $\mathcal{C}$  such that  $V_i \perp_d V_j \mid \mathcal{C}$  must be disjoint from  $\text{IMD}(V_i, V_j)$ .

Clearly, an IPA conditioning set  $\mathcal{C}$  will need to avoid the immoral descendants  $\text{IMD}(V_i, V_j)$  in order to preserve  $V_i \perp_d V_j \mid \mathcal{C}$ . Lemma 5 will show that  $\mathcal{S}_i, \mathcal{S}_j$  must also avoid  $\text{IMD}(V_i, V_j)$ .

**Lemma 5.** All IPAs for  $V_i, V_j$  are disjoint from the  $\text{IMD}(V_i, V_j)$ . That is,  $\text{IMD}(V_i, V_j) \cap \mathcal{S}_i^+ = \emptyset$  and  $\text{IMD}(V_i, V_j) \cap \mathcal{S}_j^+ = \emptyset$  for all IPAs  $(\mathcal{S}_i^+, \mathcal{S}_j^+)$  of  $(V_i, V_j)$ .

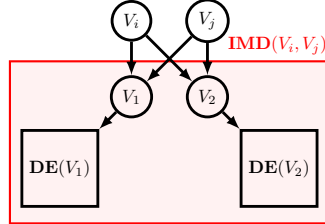


Figure 2: An illustration of an FP edge after Phase I due to a large set of immoral descendants. The population variable  $U$  is omitted to avoid clutter. While  $V_i$  and  $V_j$  are  $d$ -separated by  $\mathcal{C} = \emptyset$  no IPA can be made because all of the leftover vertices are immoral descendants.

This illustrates that FP edges can occur as pairs of vertices with too many immoral descendants, leaving no vertices to form IPAs (shown in Figure 2).

#### 3.1.2 Using non-descendants to form IPAs

Notice that the immoral descendants of a pair of vertices are always descendants of both  $V_i$  and  $V_j$ . To simplify our analysis, we focus on the existence of IPAs that are disjoint from the entire set of descendants. This allows us to show that FP edges only occur between “early vertices.”

**Definition 5.** We define the early vertices,

$$\mathbf{H} := \{V \in \mathbf{V} \text{ s.t. } |\overline{\text{DE}}(V)| < (2 + \Delta^2)(\lceil \lg(k) \rceil + 1)\}.$$

**Lemma 6.** After Phase I (Algorithm 1), all of the false positive edges lie within the early vertices. More formally,  $\mathbf{E}_1 \setminus \mathbf{E} \subseteq \mathbf{H} \times \mathbf{H}$ .

**Observation 2.**  $|\mathbf{H}| \leq (2 + \Delta^2)\lceil \lg(k) \rceil$  and the maximum degree of  $\mathcal{G}_1$  is bounded by  $|\mathbf{H}|$ .

### 3.2 Phase II: Handle FP Edges

Recall that the marginal probability distribution cannot use independence tests to discover non-adjacency because latent variable  $U$  confounds all of the independence properties. An important observation is that the within-source distribution  $\Pr(\mathbf{V} \mid u)$  would not suffer from this limitation because it would allow us to condition on separating sets that include unobserved  $U$ .

Phase II will make use of this observation by selecting subsets of variables  $\mathbf{T} \subseteq \mathbf{V}$  on which to obtain  $\Pr(\mathbf{T} \mid u)$  using techniques from discrete mixture models. We will then apply regular conditional independence tests on the recovered  $\Pr(\mathbf{T} \mid u)$  to detect FP edges. We will use a separate  $\mathbf{T}_{ij} \ni V_i, V_j$  coarsening to verify each edge  $(V_i, V_j) \in \mathbf{E}_1$ , though this process can likely be optimized further.

The primary result on mixture model identifiability is given by E. S. Allman [2009] as a direct consequence of a result by Kruskal [1977].

**Lemma 7** (E. S. Allman [2009]). *Consider the discrete mixture source  $U \in \{1, \dots, k\}$  and discrete variables  $X_1, X_2, X_3$  with cardinality  $\kappa_1, \kappa_2, \kappa_3$  respectively and  $X_1 \perp\!\!\!\perp X_2 \perp\!\!\!\perp X_3 \mid U$ . The mixture is generically identifiable (with Lebesgue measure 1 on the parameter space) if*

$$\min(\kappa_1, k) + \min(\kappa_2, k) + \min(\kappa_3, k) \geq 2k + 2.$$

We can again use coarsening to form  $X_i$  with large enough  $\kappa_i$ . The conditions for identifiability are therefore quite mild - Phase I only needs to uncover enough sparsity to  $d$ -separate three sufficiently large independent coarsenings, one of which will be  $\mathbf{T}_{ij}$ . Conveniently, the constrained nature of our FP edges means that the graph  $\mathcal{G}_1$  is sufficiently sparse to allow the construction of this setting.

$\mathbf{T}_{ij}$  must be designed to include enough information to discover a nonadjacency between  $V_i, V_j$ . In other words, we need to ensure that  $\mathbf{T}_{ij}$  contains a separating set  $\mathbf{C} \subset \mathbf{T}_{ij}$  such that  $V_i \perp\!\!\!\perp_d^{\mathcal{G}} V_j \mid \mathbf{C}$ . It turns out that augmenting  $V_i, V_j$  with their distance-1 neighborhood is enough to guarantee this requirement.

**Definition 6.** Given vertices  $V_i, V_j$ , let  $\mathbf{T}_{ij}$  be the set containing  $V_i, V_j$  and all vertices that are distance 1 in  $\mathcal{G}_1$  from  $V_i$  or  $V_j$ .

**Lemma 8.** *If vertices  $V_i, V_j$  are nonadjacent, the set  $\mathbf{T}_{ij}$  contains a valid separating set  $\mathbf{C} \subseteq \mathbf{T}_{ij}$  such that  $V_i \perp\!\!\!\perp_d V_j \mid \mathbf{C}$ .*

Lemma 8 guarantees that the conditional probability distribution  $\Pr(\mathbf{T}_{ij} \mid u)$  has sufficient information to verify or falsify the adjacency of  $V_i$  and  $V_j$ .

The rest of the construction of the  $k$ -MixProd instances is left to Appendix D. Generally, it involves ensuring that the recovered  $\mathcal{G}_1$  from Phase I is sparse enough to  $d$ -separate all  $\mathbf{T}_{ij}$  from two other supervariables of sufficient cardinality. The procedure is outlined by Algorithm 2 and then Algorithm 3 performs the actual correction with the statistics recovered from  $k$ -MixProd oracles. Lemma 9 summarizes the results proved in Appendix D.

**Lemma 9.** *Phase II requires  $\Omega(\Delta^3 \log(k))$  vertices and solves  $k$ -MixProd  $\mathcal{O}(k|\mathbf{E}|2^{\Delta^2})$  times.*

## 4 Empirical Results

The algorithm is successful when enough data is gathered, as proved by our theoretical results. We now employ three empirical tests to show the superiority of our derived hypothesis-based rank test as well as investigate the sensitivity of Phase I. The graph structures of our tests are described here, with the details of the structural equations left to Appendix E. The results of the experiments are given and analysis is also deferred to Appendix E.

### 4.1 Test 1: Rank Hypothesis Test vs. Singular Values

We begin with a comparison of the test developed in Section 2.2 to a naive thresholding of singular values as in Anandkumar et al. [2012]. To study the differences between these tests, we generate data from two observed subgraphs.

1. “Connected”  $\mathcal{G}^c$ :  $V_1 \rightarrow V_2 \rightarrow V_3 \rightarrow V_4$



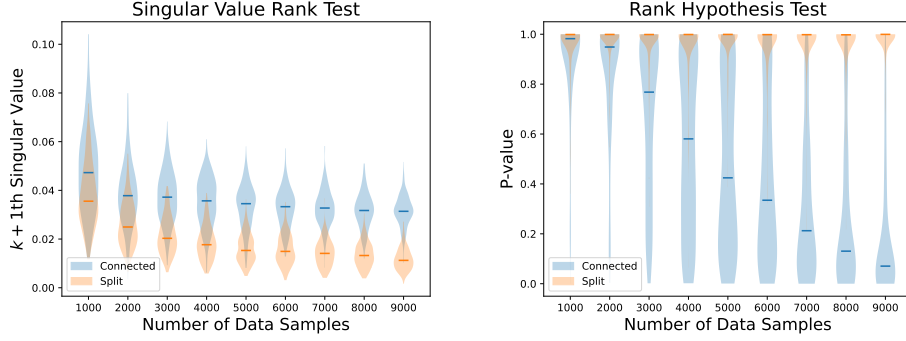


Figure 3: The results of Test 1.

2. “Split”  $\mathcal{G}^s$ :  $V_1 \rightarrow V_2 \ V_3 \rightarrow V_4$

If we coarsen our vertices into  $\mathcal{S}_i^+ = \{V_1, V_2\}$  and  $\mathcal{S}_j^+ = \{V_3, V_4\}$ , then these two DAGs differ in that  $\mathcal{S}_i^+ \not\perp_d^{\mathcal{G}^c} \mathcal{S}_j^+$  and  $\mathcal{S}_i^+ \perp_d^{\mathcal{G}^s} \mathcal{S}_j^+$ . We note that this is a challenging test, as the connection between the two partitions is only driven by the  $X_2 \rightarrow X_3$  arrow.

We varied the number of samples from these distributions from 1000 to 9000 and studied the distributions of the two reported p-values and  $k + 1$ th singular values across 200 runs. The results are reported in Figure 3, showing that the hypothesis test has significant difference in p-values beyond 4000 samples (relative to the difference in the  $k + 1$ th singular values).

4.2 Test 2: Recovering a “Y” Graph

The second test is a simple recovery test on a 7 vertex graph in which two disconnected parents form a child, with a series of descendants. We sample 10,000 data points and test with a p-value of .0005 – i.e. we remove edges when we get a p-value of .9995 in our rank test (a value that is motivated by knock-on effects and the concentration of the “split” graph results in Test 1). We report our results from 100 different tests (and implicitly show the tested graph) in Figure 4.

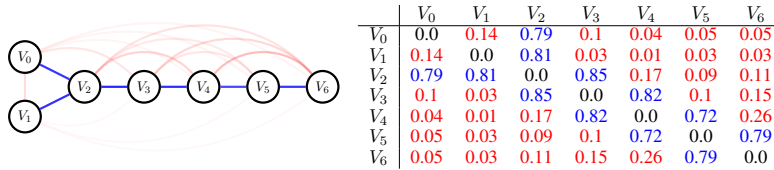


Figure 4: Results from Test 2. In blue, we show correctly returned edges. In red, we show edges that were returned which are **not** in the true model. The opacity of the lines show the percentage of the time that the edge was returned (ideally, we would want faint red lines and strong blue lines). To the right of the graph, we show a table of the frequency of returning the edge colored according to the same scheme.

4.3 Test 3: Many Graphs with Varying Density

In our third test, we explore the role that graph density plays in accurately detecting graph adjacency. For this test, we sample random Erdős-Renyi undirected graph structures on 7 vertices and orient them according to a random permutation of the edges. We vary the probability of edge-occurrence in our graphs from .1 to .9 in .1 increments, sampling 20 graph structures for each. Among these graphs we draw 10,000 datapoints and study the role of maximum in-degree and total number of edges on the percentage of correctly recovered edges (p-value .0005 again). The results are given in Figure 5.

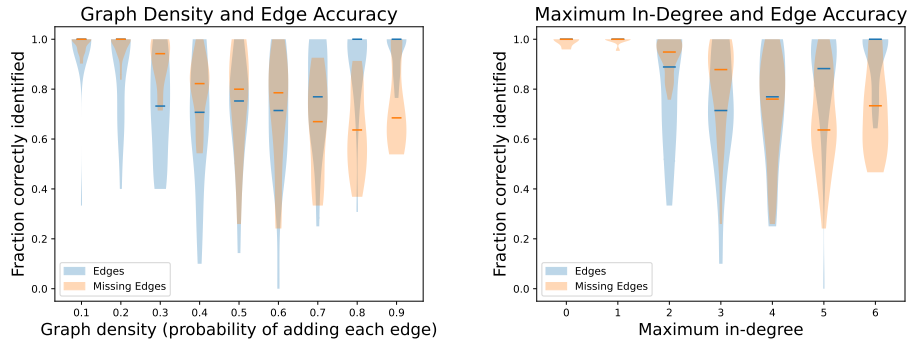


Figure 5: The results of Test 3. Horizontal ticks represent the median accuracy for recovering edges (blue) or lack of edges (orange). A violin plot is also shown, representing the density of results over 20 iterations at each  $p$  (probability of adding an edge).

## References

- Silvia Acid and Luis M De Campos. An algorithm for finding minimum d-separating sets in belief networks. In *Proceedings of the Twelfth international conference on Uncertainty in artificial intelligence*, pages 3–10, 1996.
- Raj Agrawal, Chandler Squires, Neha Prasad, and Caroline Uhler. The DeCAMFounder: nonlinear causal discovery in the presence of hidden variables. *Journal of the Royal Statistical Society Series B: Statistical Methodology*, page qkad071, 07 2023. ISSN 1369-7412. doi: 10.1093/jrsssb/qkad071. URL <https://doi.org/10.1093/jrsssb/qkad071>.
- A. Anandkumar, D. Hsu, F. Huang, and S. M. Kakade. Learning high-dimensional mixtures of graphical models. *arXiv preprint arXiv:1203.0697*, 2012.
- Ruichu Cai, Zhiyi Huang, Wei Chen, Zhifeng Hao, and Kun Zhang. Causal discovery with latent confounders based on higher-order cumulants. *arXiv preprint arXiv:2305.19582*, 2023.
- Federico Castanedo. A review of data fusion techniques. *The scientific world journal*, 2013, 2013.
- K. Chaudhuri and S. Rao. Learning mixtures of product distributions using correlations and independence. In *Proc. 21st Ann. Conf. on Learning Theory - COLT*, pages 9–20. Omnipress, 2008. URL <http://colt2008.cs.helsinki.fi/papers/7-Chaudhuri.pdf>.
- S. Chen and A. Moitra. Beyond the low-degree algorithm: mixtures of subcubes and their applications. In *Proc. 51st Ann. ACM Symp. on Theory of Computing*, pages 869–880, 2019. doi: 10.1145/3313276.3316375.
- M. Cryan, L. Goldberg, and P. Goldberg. Evolutionary trees can be learned in polynomial time in the two state general Markov model. *SIAM J. Comput.*, 31(2):375–397, 2001. doi: 10.1137/S0097539798342496.
- Jingqiu Ding, Tommaso d’Orsi, Chih-Hung Liu, David Steurer, and Stefan Tiegel. Fast algorithm for over-complete order-3 tensor decomposition. In *Conference on Learning Theory*, pages 3741–3799. PMLR, 2022.
- J. A. Rhodes E. S. Allman, C. Matias. Identifiability of parameters in latent structure models with many observed variables. *Ann. Statist.*, 37(6A):3099–3132, 2009. doi: 10.1214/09-AOS689.
- J. Feldman, R. O’Donnell, and R. A. Servedio. Learning mixtures of product distributions over discrete domains. *SIAM J. Comput.*, 37(5):1536–1564, 2008. doi: 10.1137/060670705.
- Y. Freund and Y. Mansour. Estimating a mixture of two product distributions. In *Proc. 12th Ann. Conf. on Computational Learning Theory*, pages 53–62, July 1999. doi: 10.1145/307400.307412.
- Benjamin Frot, Preetam Nandy, and Marloes H Maathuis. Robust causal structure learning with some hidden variables. *Journal of the Royal Statistical Society Series B: Statistical Methodology*, 81(3):459–487, 2019.
- Spencer L Gordon, Bijan Mazaheri, Yuval Rabani, and Leonard J Schulman. Source identification for mixtures of product distributions. In *Proc. 34th Ann. Conf. on Learning Theory - COLT*, volume 134 of *Proc. Machine Learning Research*, pages 2193–2216. PMLR, 2021. URL <http://proceedings.mlr.press/v134/gordon21a.html>.

- Spencer L Gordon, Erik Jahn, Bijan Mazaheri, Yuval Rabani, and Leonard J Schulman. Identification of mixtures of discrete product distributions in near-optimal sample and time complexity. *arXiv preprint arXiv:2309.13993*, 2023a.
- Spencer L Gordon, Bijan Mazaheri, Yuval Rabani, and Leonard J Schulman. Causal inference despite limited global confounding via mixture models. In *2nd Conference on Causal Learning and Reasoning*, 2023b.
- M. Kearns, Y. Mansour, D. Ron, R. Rubinfeld, R. Schapire, and L. Sellie. On the learnability of discrete distributions. In *Proc. 26th Ann. ACM Symp. on Theory of Computing*, pages 273–282, 1994. doi: 10.1145/195058.195155.
- Joseph B Kruskal. Three-way arrays: rank and uniqueness of trilinear decompositions, with application to arithmetic complexity and statistics. *Linear algebra and its applications*, 18(2):95–138, 1977.
- Steffen L Lauritzen, A Philip Dawid, Birgitte N Larsen, and H-G Leimer. Independence properties of directed markov fields. *Networks*, 20(5):491–505, 1990.
- Ankur Moitra. An almost optimal algorithm for computing nonnegative rank. *SIAM Journal on Computing*, 45(1):156–173, 2016.
- Judea Pearl. *Probabilistic reasoning in intelligent systems: networks of plausible inference*. Morgan kaufmann, 1988.
- Judea Pearl. *Causality*. Cambridge university press, 2009.
- Jonas Peters, Dominik Janzing, and Bernhard Schölkopf. *Elements of causal inference: foundations and learning algorithms*. The MIT Press, 2017.
- Yuval Rabani, Leonard J Schulman, and Chaitanya Swamy. Learning mixtures of arbitrary distributions over large discrete domains. In *Proc. 5th Conf. on Innovations in Theoretical Computer Science*, pages 207–224, 2014. doi: 10.1145/2554797.2554818.
- Zaka Ratsimalahelo. Rank test based on matrix perturbation theory. Technical report, EERI Research Paper Series, 2001.
- Thomas Richardson and Peter Spirtes. Ancestral graph markov models. *The Annals of Statistics*, 30(4):962–1030, 2002.
- Basil Saeed, Snigdha Panigrahi, and Caroline Uhler. Causal structure discovery from distributions arising from mixtures of dags. In *International Conference on Machine Learning*, pages 8336–8345. PMLR, 2020.
- P. Spirtes, C. Glymour, R. Scheines, S. Kauffman, V. Aimale, and F. Wimberly. Constructing Bayesian network models of gene expression networks from microarray data. 2000a.
- Peter Spirtes. An anytime algorithm for causal inference. In *International Workshop on Artificial Intelligence and Statistics*, pages 278–285. PMLR, 2001.
- Peter Spirtes, Clark Glymour, Richard Scheines, Peter Spirtes, Clark Glymour, and Richard Scheines. Discovery algorithms for causally sufficient structures. *Causation, prediction, and search*, pages 103–162, 1993.
- Peter Spirtes, Clark N Glymour, and Richard Scheines. *Causation, prediction, and search*. MIT press, 2000b.
- Chandler Squires and Caroline Uhler. Causal structure learning: A combinatorial perspective. *Foundations of Computational Mathematics*, 23(5):1781–1815, 2023.
- B. Tahmasebi, S. A. Motahari, and M. A. Maddah-Ali. On the identifiability of finite mixtures of finite product measures. (Also in “On the identifiability of parameters in the population stratification problem: A worst-case analysis,” Proc. ISIT’18 pp. 1051-1055), 2018. URL <https://arxiv.org/abs/1807.05444>.

## A D-separation

We will rely on the concepts of **d-separation**, **active paths**, and **separating sets**. Active paths are defined relative to sets of variables to be conditioned on (“conditioning sets”).

A key concept in active paths is that of a collider,  $C$ , which takes the form  $V_1 \rightarrow C \leftarrow V_2$  along an undirected path. Undirected paths through unconditioned variables with no colliders are considered active because they can “carry dependence” from one end of the path to the other. If a non-collider along one of these non-collider paths is conditioned on, then the path is inactive.

Collider steps of paths behave in the opposite fashion: paths with an unconditioned collider are inactive, whereas conditioning on a collider or any descendant of that collider “opens” the active path.

When two variables have an active path between them, we say that they are d-connected. If there are no active paths between the variables, we say they are d-separated. A separating set between two variables is a set of variables which, when conditioned on, break all active paths between those variables. While only loosely described here, a full precise definition of d-separation can be found in Pearl [1988] and Pearl [2009] (for a more extensive study).

Pearl [1988] uses structural causal models to justify the *local Markov condition*, which means that d-separation always implies independence and allows DAG structures to be factorized. It is possible that two d-connected variables by chance exhibit some unexpected *statistical independence*. This complication is often assumed away using “faithfulness” [Spirtes et al., 2000b], which ensures that d-connectedness implies statistical dependence. Together, the local Markov condition and faithfulness give a correspondence statistical dependence and the graphical conditions of the causal DAG which can be leveraged for causal structure learning.

The following fact will be useful when building separating sets.

**Lemma 10** (Pearl [2009]). *If vertices  $V_i, V_j$  are nonadjacent in  $\mathcal{G}$ , either  $\text{PA}^{\mathcal{G}}(V_i)$  or  $\text{PA}^{\mathcal{G}}(V_j)$  are a valid separating set for  $V_i, V_j$ .*

We will often want to bound the cardinality of separating sets relative to the degree bound of the graph ( $\Delta$ ). When dealing with a separating set between two vertices  $V_i, V_j$ , Lemma 10 implies a simple upper bound of  $\Delta$ . Separating sets for *sets* (or coarsenings) of vertices are significantly more complicated because conditioning may d-separate some pairs of vertices while d-connecting others.

To unify the treatment of separating sets, we will make use of **moral graphs**, which can be thought of as undirected equivalents of DAGs [Lauritzen et al., 1990]. We will denote the moral graph of  $\mathcal{G}$  as  $\mathcal{G}^{(m)}$ . To transform  $\mathcal{G}$  into  $\mathcal{G}^{(m)}$ , we add edges between all immoralities, i.e. nonadjacent vertices with a common child, sometimes called an unshielded collider. After this, we change all directed edges to undirected edges.

A very useful fact from Lauritzen et al. [1990] (also Eq. 1 in Acid and De Campos [1996]) is that all separating sets  $C \subseteq V$  for  $S, S' \subseteq V$  in  $\mathcal{G}$  are also separating sets in  $(\mathcal{G}[\text{AN}^+(S \cup S' \cup C)])^{(m)}$ . This transforms complicated active path analysis into simple connectedness arguments on undirected moral graphs (of special subgraphs of  $\mathcal{G}$ ). A convenient consequence of this transformation, which we will use throughout the paper, is Lemma 11.

**Lemma 11.** *If  $\mathcal{G} = (V, E)$  has degree bound  $\Delta$ , then the size of a separating set between  $S, S' \subseteq V$  is no larger than  $\min(|S|, |S'|)\Delta^2$ .*

Lemma 11 is a consequence of the maximum increase in the degree of the moral graph.

*Proof.* A key observation is that the moral graph of a subgraph of  $\mathcal{G}$  has no additional edges relative to  $\mathcal{G}^{(m)}$ . That is, if  $\mathcal{G}[\mathbf{W}] = (W, F)$  is a subgraph of  $\mathcal{G} = (V, E)$  then the corresponding edge-sets of the moral graphs obey  $F^{(m)} \subseteq E^{(m)}$  because adding vertices cannot have invalidated any previously contained immoralities.

Abbreviate  $(\mathcal{G}[\text{AN}^+(S \cup S' \cup C)])^{(m)}$  as  $\mathcal{G}_C^{(m)}$ . Even though we do not know what  $C$  is, we know that the 1-neighborhood of  $S$  in  $\mathcal{G}_C^{(m)}$  suffices as a separating set.  $\mathcal{G}^{(m)}$  has all of the edges of  $\mathcal{G}_C^{(m)}$ , so

$$\text{NB}_1^{\mathcal{G}_C^{(m)}}(S) \subseteq \text{NB}_1^{\mathcal{G}^{(m)}}(S). \quad (9)$$

Note that  $\text{NB}_1^{\mathcal{G}^{(m)}}(\mathcal{S})$  is not necessarily a separating set for  $\mathcal{S}, \mathcal{S}'$  in  $\mathcal{G}^{(m)}$ , in fact it may include some vertices in  $\mathcal{S}$  itself. However, the size of the separating set is bounded by  $|\text{NB}_1^{\mathcal{G}^{(m)}}(\mathcal{S})|$ , which is no larger than  $|\mathcal{S}|\Delta^2$ . As we chose  $\mathcal{S}$  arbitrarily, this bound also holds for  $\mathcal{S}'$ .  $\square$

Another helpful result from moral graphs is Lemma 12, which will help us when we prove the existence of separating sets.

**Lemma 12** (Corollary of Theorem 1 in Acid and De Campos [1996]). *For DAG  $\mathcal{G} = (\mathbf{V}, \mathbf{E})$ , and  $\mathcal{S}, \mathcal{S}' \subseteq \mathbf{V}$ , separating sets  $\mathcal{S}, \mathcal{S}'$  in  $(\mathcal{G}[\text{AN}^+(\mathcal{S} \cup \mathcal{S}')])^{(m)}$  are also separating sets in  $\mathcal{G}$ .*

## B Identifying Mixtures of Discrete Products

The main tool used in Gordon et al. [2023b] is a solution to identifying discrete  $k$ -mixtures of product distributions ( $k$ -MixProd) - i.e.  $\mathbf{X} = X_1, \dots, X_n$  and latent global confounder or “source”  $U$  such that  $X_i \perp\!\!\!\perp X_j \mid U$  for all  $i, j$ . The key complexity parameter for identifiability is  $k$ , the cardinality of the support of  $U$ .<sup>5</sup>

At its core,  $k$ -MixProd shows how coincidences of multiple independent events reveal information about their confoundedness. Of course, it is possible for  $U$  with sufficiently large  $k$  to completely control the distribution on  $\mathbf{X}$ . For example, for binary  $X_i \in \{0, 1\}$ , a cardinality of  $k = 2^n$  would be sufficient to assign each binary sequence in  $\mathbf{X}$  to a latent class in  $U$ . Such a powerful  $U$  could generate *any* desired probability distribution on  $\mathbf{X}$  by simply controlling the probability distribution on  $U$ . Limiting  $k$ , however, limits the space of marginal probability distributions on  $\mathbf{X}$ , eventually giving rise to identifiability.

Under a cardinality bound  $k$  on the support of  $U$ , E. S. Allman [2009] showed that  $n \geq \Omega(\log(k))$  is sufficient for the generic identification of  $k$ -MixProd. In other words, other than a Lebesgue measure 0 set of exceptions, most instances of  $k$ -MixProd have a one-to-one correspondence with their observed statistics (the probability distribution on  $\mathbf{X}$  marginalized over  $U$ ) and generating model (up to a set of  $k!$  models with permuted labels of  $U$ ).

For guaranteed identifiability, Tahmasebi et al. [2018] demonstrated that a linear lower bound ( $n \geq 2k - 1$ ), in conjunction with a separation condition in the distributions of  $X_i \mid U$ , is sufficient to guarantee identifiability. The best known algorithm for identification is given in Gordon et al. [2023a], which nearly matches the known lower bounds for sample complexity. This paper will use the result from E. S. Allman [2009], but our methods easily extend to stronger identifiability conditions with modifications in the sparsity requirements.

## C Further Runtime Discussion

The non-negative rank of a  $k + 1 \times k + 1$  matrix (as used for our algorithm) can be solved in time  $k^{\mathcal{O}(k^2)}$  [Moitra, 2016]. In the absence of non-negative rank tests, Anandkumar et al. [2012] demonstrated that regular rank tests generally work well in place of non-negative rank tests in practice. We will develop a hypothesis test for matrix-rank that requires  $\mathcal{O}(k^6)$  operations to invert a  $(k + 1)^2 \times (k + 1)^2$  covariance matrix of the estimated elements of our  $k + 1 \times k + 1$  matrix.

Our solution also requires solving  $k$ -MixProd on 3 variables of cardinality  $\mathcal{O}(k)$ , which corresponds to decomposing a  $\mathcal{O}(k) \times \mathcal{O}(k) \times \mathcal{O}(k)$  tensor into rank 1 components. When the rank of such a tensor is known to be linear in  $k$ , this decomposition can be solved in  $\mathcal{O}(k^{6.05})$  [Ding et al., 2022], though Gordon et al. [2021] showed that the problem generally suffers from instability, with sample complexity exponential in  $k$ . This step may be considered optional, as it is used to refine a small number of “false-positive” adjacencies confined to a provably small subset of the DAG.

## D Utilizing $\mathcal{G}_1$ to set up $k$ -MixProd

The first step to recovering  $\Pr(\mathbf{T}_{ij} \mid u)$  will be to select some  $\mathbf{Z}_{ij}$  and recover  $\Pr(\mathbf{T}_{ij} \mid u, \mathbf{z}_{ij})$  using instances of  $k$ -MixProd induced on the conditional probability distribution  $\Pr(\mathbf{V} \mid \mathbf{z}_{ij})$ . Recall

<sup>5</sup>We will refer to the cardinality of the support of discrete random variables as their cardinality.

that  $k$ -MixProd requires three independent variables of sufficient cardinality. Hence, we must find  $\mathbf{X}_1, \mathbf{X}_2, \mathbf{T}_{ij}$  which are sufficiently large, and d-separated from each other by  $\mathbf{Z}_{ij}$  in  $\mathcal{G}$ . See Figure 6 for an example.

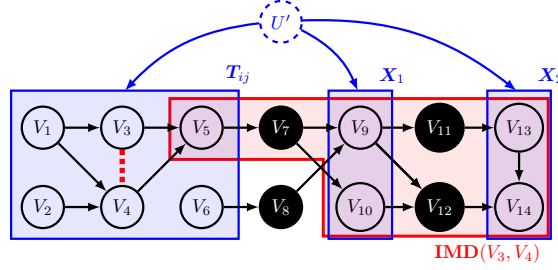


Figure 6: The given graph has an FP edge between  $V_3$  and  $V_4$ , indicated by a dashed line, caused by a large set of immoral descendants (shown in red). Conditioning on  $V_7, V_{11}, V_{12}$  creates an instance of  $k$ -MixProd on  $\mathbf{T}_{ij}, \mathbf{X}_1, \mathbf{X}_2$ . Notice that  $V_7, V_{11}, V_{12}$  are all in  $\text{IMD}(V_3, V_4)$ , which means that the  $\Pr(\mathbf{T}_{ij} \mid V_7, V_{11}, V_{12}, u')$  recovered by  $k$ -MixProd will not be sufficient for detecting the FP edge. This obstacle will be solved in Subsection D.2.

Of course we have access to  $\mathcal{G}_1$ , not  $\mathcal{G}$ .  $\mathcal{G}_1$  contains no orientations<sup>6</sup> and may contain extra false-positive edges. We will need to build a conditioning set  $\mathbf{Z}_{ij}$  that achieves a guaranteed instance of  $k$ -MixProd nonetheless. While Markov boundaries cannot be computed without  $\mathcal{G}$ , we can easily use  $\mathcal{G}_1$  to find a superset that *contains* the Markov boundary of a given vertex.

**Lemma 13.** *The 2-neighborhood of  $\mathbf{X} \subseteq \mathbf{V}$  in  $\mathcal{G}_1$  contains  $\text{MB}^{\mathcal{G}}(\mathbf{X})$ .*

*Proof.* The distance between  $X \in \mathbf{X}$ , and  $V \in \mathbf{V}$  in  $\mathcal{G}_1$  is less than or equal to the distance in  $\mathcal{G}$ , because  $\mathbf{E}_1 \supseteq \mathbf{E}$ . This means that the 2-neighborhood of  $\mathbf{X}$  in  $\mathcal{G}_1$  includes the 2-neighborhood of  $\mathbf{X}$  in  $\mathcal{G}$ . Furthermore because all vertices in  $\text{MB}^{\mathcal{G}}(\mathbf{X})$  are distance  $\leq 2$  from at least one  $X \in \mathbf{X}$ , we have that  $\text{MB}^{\mathcal{G}}(\mathbf{X})$  is contained in the 2-neighborhood of  $\mathbf{X}$  in  $\mathcal{G}_1$ .  $\square$

The sparsity of  $\mathcal{G}_1$  will dictate the number of necessary vertices to successfully set up  $k$ -MixProd. We will want to limit the size of  $\mathbf{Z}_{ij}$  as much as possible. Fortunately, the bounds on the size of  $\mathbf{H}$  mean that *most* of  $\mathcal{G}_1$  is degree bounded by  $\Delta$ . We will avoid large degree vertices in  $\mathbf{H}$  by strategically selecting  $\mathbf{X}_1, \mathbf{X}_2$  with the smallest 2-neighborhoods.  $\mathbf{Z}_{ij} = \text{MB}(\mathbf{X}_1) \cup \text{MB}(\mathbf{X}_2)$  will be sufficient to d-separate all three vertices, so we need not worry about potentially large degree in  $\mathbf{T}_{ij}$ . This process is described by Algorithm 2.

#### Algorithm 2: Formation of $k$ -MixProd Instances

**Input:** Two vertices  $V_i, V_j \in \mathbf{V}$  and  $\mathcal{G}_1 = (\mathbf{V}, \mathbf{E}_1)$  from the output of Algorithm 1.

**Output:**  $\mathbf{T}_{ij}, \mathbf{X}_1, \mathbf{X}_2$  and  $\mathbf{Z}_{ij}$  such that  $\mathbf{T}_{ij} \perp\!\!\!\perp_d \mathbf{X}_1 \perp\!\!\!\perp_d \mathbf{X}_2 \mid \mathbf{Z}_{ij}$ .

Let  $\mathbf{T}_{ij} = \{V_i, V_j\} \cup \text{NB}_1^{\mathcal{G}_1}(V_i) \cup \text{NB}_1^{\mathcal{G}_1}(V_j)$ .

$\mathbf{V}' \leftarrow \mathbf{V} \setminus (\mathbf{T}_{ij} \cup \text{NB}_2(\mathbf{T}_{ij}))$

$\mathbf{X}_1, \mathbf{X}_2$  all begin as empty sets.

**while**  $2^{|\mathbf{X}_1|} + 2^{|\mathbf{X}_2|} < 2k + 2 - \min(k, 2^{|\mathbf{T}_{ij}|})$  **do**

    | Add  $V \in \mathbf{V}' \setminus (\text{NB}_2(\mathbf{X}_2) \cup \mathbf{X}_2)$  to  $\mathbf{X}_1$ .

    | Add  $V \in \mathbf{V}' \setminus (\text{NB}_2(\mathbf{X}_1) \cup \mathbf{X}_1)$  to  $\mathbf{X}_2$ .

**end**

$\mathbf{Z}_{ij} \leftarrow \text{NB}_2(\mathbf{X}_1) \cup \text{NB}_2(\mathbf{X}_2)$ .

**Lemma 14.** *Algorithm 2 terminates successfully (without running out of vertices in  $\mathbf{V}'$ ) with  $\Omega(\Delta^3 \log(k))$  vertices.*

*Proof.* The algorithm designates vertices in  $\mathbf{V}$  into the following sets and succeeds so long as those sets are disjoint.

<sup>6</sup>It is, in principle, possible to orient immoralities within  $\mathcal{G}_1$  at this stage, but this gives no complexity improvements.

1.  $\mathbf{X}_1$  and  $\mathbf{X}_2$
2.  $\text{NB}_2(\mathbf{X}_1), \text{NB}_2(\mathbf{X}_2)$
3.  $\mathbf{T}_{ij}$
4.  $\text{NB}_1(\mathbf{T}_{ij})$

$|\mathbf{T}_{ij}| \geq 2$  and  $k \geq 2$ , so the number of vertices added to  $\mathbf{X}_1, \mathbf{X}_2$  in the loop of Algorithm 2 is at most  $\lceil \lg(2k + 2 - 2) \rceil < \lg(k) + 2$ . To bound the 2-neighborhood, we notice that we cannot easily apply our degree bound of  $\Delta$  because  $\mathbf{H}$  could be a clique in  $\mathcal{G}_1$  (from FP edges). Instead, we bound

$$|\text{NB}_2(\mathbf{X}_1) \cup \text{NB}_2(\mathbf{X}_2) \cup \mathbf{X}_1 \cup \mathbf{X}_2| \leq \Delta^2 |\mathbf{X}_1 \cup \mathbf{X}_2| + \Delta |\mathbf{H}| \quad (10)$$

because the distance 1 neighborhood could include all of  $\mathbf{H}$  but all additional neighborhoods are bounded by  $\Delta$ .  $|\mathbf{H}|$  is  $\mathcal{O}(\Delta^2 \log(k))$  by Observation 2, so this bound is  $\mathcal{O}(\Delta^3 \log(k))$ .

The size of  $\mathbf{T}_{ij}$  is the largest when including  $V_i$  or  $V_j$  in  $\mathbf{H}$ , for which  $\text{NB}_1(V_i)$  could be all of  $\mathbf{H}$  and  $\text{NB}(V_i)$  then necessarily falls outside of  $\mathbf{H}$ . This worst case gives

$$|\mathbf{T}_{ij}| \leq |\mathbf{H}| + \Delta^2. \quad (11)$$

which is  $\mathcal{O}(\Delta^2 \log(k))$ . Expanding to the 1 neighborhood picks up another factor of  $\Delta$ , bringing us again to  $\mathcal{O}(\Delta^3 \log(k))$ . □

### D.1 Aligning multiple $k$ -MixProd runs

$k$ -MixProd distributions are symmetric with respect to the  $k!$  permutations on the label of their source. For this reason, there is no guarantee that multiple calls to a  $k$ -MixProd solver will return the same permutation of source labels.

To solve this, Gordon et al. [2023b] noticed that any two solutions to  $k$ -MixProd problems that share the same conditional probability distribution for at least one “alignment variable” can be “aligned” by permuting the source labels until the distributions on that variable match up. We will only need alignment along runs for different assignments to each  $\mathbf{Z}_{ij}$ , used in the next section. Explicitly, two assignments  $\mathbf{z}_{ij}$  and  $\mathbf{z}'_{ij}$ , need least one  $\mathbf{X}^* \in \{\mathbf{T}_{ij}, \mathbf{X}_1, \mathbf{X}_2\}$  such that  $\text{mb}_{\mathbf{z}_{ij}}(\mathbf{X}^*)$  and  $\text{mb}_{\mathbf{z}'_{ij}}(\mathbf{X}^*)$  are the same, in order for alignability to be satisfied.

To align sets of  $k$ -MixProd results which are not all pairwise alignable, Gordon et al. [2023b] introduced the concept of an “alignable set of runs” for which chains of alignable pairs create allow alignability.

**Lemma 15.** *The set of  $k$ -MixProd instances on the same  $\mathbf{T}_{ij}, \mathbf{X}_1, \mathbf{X}_2$  with all possible assignments  $\mathbf{z}_{ij}$  to  $\mathbf{Z}_{ij}$  is alignable.*

*Proof.* Any two runs with assignments  $\mathbf{z}_{ij}$  and  $\mathbf{z}'_{ij}$  that differ in their assignment to only one variable are alignable. Therefore, any two non-alignable runs can be aligned using a chain of Hamming-distance one alignments. □

### D.2 Recovering the unconditioned within-source distribution

After all our calls to the  $k$ -MixProd oracle, we have access to  $\Pr(\mathbf{T}_{ij} \mid u, \mathbf{z}_{ij})$  and  $\Pr(u \mid \mathbf{z}_{ij})$  for every assignment  $\mathbf{z}_{ij}$  and  $u$ .  $\Pr(\mathbf{T}_{ij} \mid u, \mathbf{z}_{ij})$  is insufficient to determine the adjacency of  $V_i, V_j$  because  $\mathbf{Z}_{ij}$  may contain vertices in the immoral descendants of  $V_i, V_j$ , prohibiting the discovery of a separating set within  $\mathbf{T}_{ij}$ .

Instead, we must recover  $\Pr(\mathbf{T}_{ij} \mid u)$ , which is not conditioned on  $\mathbf{Z}_{ij}$ . To do this, we can apply the law of total probability over all possible assignments to  $\mathbf{Z}_{ij}$ .

$$\Pr(\mathbf{T}_{ij} \mid u) = \sum_{\mathbf{z}_{ij}} \Pr(\mathbf{z}_{ij} \mid u) \Pr(\mathbf{T}_{ij} \mid \mathbf{z}_{ij}, u) \quad (12)$$

We can obtain  $\Pr(\mathbf{z}_{ij} | u)$  by using Bayes rule on the  $k$ -MixProd output,  $\Pr(u | \mathbf{z}_{ij})$ .

$$\Pr(\mathbf{z}_{ij} | u) = \frac{\Pr(u | \mathbf{z}_{ij}) \Pr(\mathbf{z}_{ij})}{\Pr(u)}. \quad (13)$$

$\Pr(\mathbf{z}_{ij})$  can be obtained by counting the frequency of  $\mathbf{z}_{ij}$  in the data. In addition,  $\Pr(u) = \sum_{\mathbf{z}_{ij}} \Pr(\mathbf{z}_{ij}) \Pr(u | \mathbf{z}_{ij})$  is computable by the law of total probability after the runs for each assignment  $\mathbf{z}_{ij}$ , have been aligned. Equivalently, we can normalize such that  $\sum_{\mathbf{z}_{ij}} \Pr(\mathbf{z}_{ij} | u) = 1$ .

**Lemma 16.** *We can compute  $\Pr(\mathbf{T}_{ij} | u)$  using known quantities,*

$$\Pr(\mathbf{T}_{ij} | u) = \frac{\sum_{\mathbf{z}_{ij}} \Pr(u | \mathbf{z}_{ij}) \Pr(\mathbf{z}_{ij}) \Pr(\mathbf{T}_{ij} | \mathbf{z}_{ij}, u)}{\sum_{\mathbf{z}_{ij}} \Pr(\mathbf{z}_{ij}) \Pr(u | \mathbf{z}_{ij})}.$$

$\Pr(\mathbf{T}_{ij} | u)$  is a completely deconfounded distribution on which we can run the PC-algorithm. The full procedure is given in Algorithm 3, in which we use Algorithm 2 followed by alignment and Lemma 16 in order to remove all of the false-positive edges from  $\mathcal{G}_1$ .

**Algorithm 3:** Phase II: Detection and correction of FP edges.

**Input:**  $\Pr(\mathbf{V})$  marginalized over  $U$ , a black box solver for  $k$ -MixProd, and  $\mathcal{G}_1 = (\mathbf{V}, \mathbf{E}_1)$  from the output of Algorithm 1.

**Output:**  $\mathcal{G}_2 = (\mathbf{V}, \mathbf{E}_2)$ , an undirected skeleton of  $\mathcal{G}$  and separating sets for nonadjacenceis (vertices not in  $\mathbf{E}_2$ ).

Start with  $\mathbf{E}_2 \leftarrow \mathbf{E}_1$ .

**for** each  $\{V_i, V_j\} \in \mathbf{E}_1$  **do**

    Retrieve  $\mathbf{T}_{ij}, \mathbf{X}_1, \mathbf{X}_2, \mathbf{Z}_{ij}$  from Algorithm 2.

**for** each assignment  $\mathbf{z}_{ij}$  **do**

        | Run the  $k$ -MixProd solver on  $\mathbf{T}_{ij}, \mathbf{X}_1, \mathbf{X}_2$  on  $\Pr(\mathbf{V} | \mathbf{z}_{ij})$ .

**end**

    Perform alignment of the  $2^{z_{ij}}$  runs to retrieve  $\Pr(\mathbf{T}_{ij} | \mathbf{Z}_{ij}, U)$ .

    Calculate  $\Pr(\mathbf{T}_{ij} | u)$  for every  $u$  using Lemma 16.

    Run PC or any other structure learning algorithm on  $\Pr(\mathbf{T}_{ij} | u)$  to find a separating set  $\mathbf{C}_{ij}$  (or verify adjacency) for  $V_i, V_j$ . If  $V_i \perp\!\!\!\perp V_j | \mathbf{C}_{ij}, u$  for all  $u$ , remove  $\{V_i, V_j\}$  from  $\mathbf{E}_2$  and store  $\mathbf{C}_{ij}$ .

**end**

**Lemma 17.** *Algorithm 3 requires solving  $k$ -MixProd  $\mathcal{O}(k|\mathbf{E}|2^{\Delta^2})$  times.*

*Proof.* This algorithm requires running  $k$ -MixProd for every possible assignment to the conditioning set  $\mathbf{D}_{ij}$ , for which we have  $|\mathbf{D}_{ij}| \leq (\lg(k) + 2)\Delta^2$  total binary variables. This gives an upper bound of  $2k2^{\Delta^2}$  runs of  $k$ -MixProd for each edge.  $\square$

## E Deferred Analysis of Experimental Results

### E.1 Details for Running Experiments

Experiments were run on a Macbook Air with an M1 processor. Running each test can be done using terminal commands in the attached folder.

```
python3 test_1_rank_experiments.py
python3 test_2_learn_structure.py
python3 test_3_change_density.py
```

Test 1 takes a few minutes to run, while test 2 and 3 can take 1-2 hours depending on how many runs are made to capture statistical significance.



## E.2 Structural Equation Setup

SCMs are made up of a graphical structure and accompanying structural equations. We focus our tests primarily on varying the graphical structure, using a standard set of structural equations on these graphs. Our  $U$  are generated using a fair coin ( $k = 2$ ), and all other vertices are Bernoulli random variables with bias  $p_V$  determined by  $V$ 's parents (including  $U$ ):

$$p_V = \frac{1 + \sum_{W \in \mathbf{PA}^{G'}(V)} W}{|\mathbf{PA}^{G'}(V)| + 2}. \quad (14)$$

Structural equations of this form have a reasonable strength between vertices that is decreased relative to in-degree.

## E.3 Test 1 Analysis

The hypothesis test does appear to remove edges more aggressively in the low-data regime – i.e. the blue curves overlap with much of the orange curve in the low-data regime. However, it is worth noting that it is almost impossible to choose a threshold for the  $k + 1$ th singular value ahead of time, whereas hypothesis tests give a meaningful interpretation to significance.

## E.4 Test 2 Analysis

This test illustrates a few things that are not revealed in our theoretical results. The first is that edges which are far-enough apart often appear independent even before conditioning on their separating sets, presumably due to their weak dependence. In these cases our algorithm will “incorrectly” remove edges between vertices too early, but still give the correct result (as with any other independence-based algorithm).

As is the case with most causal discovery algorithms, the frequency of false-positive edges tends to increase with the size of the separating set between the vertices. Vertices with a large separating set require a rank tests for each assignment to that separating set, leading to more “accidentally” dependence. These “knock-on effects” are often handled using p-value adjustments, suggesting that a smaller p-value thresholds would serve a similar purpose for our algorithm.

It is worth emphasizing this effect is dependent on the separating set for the IPA rather than the two vertices themselves. For the graph tested in Figure 4 conditioning on  $V_5$  is sufficient to induce independence between  $V_4$  and  $V_6$  in the unconfounded setting. In the presence of a global confounder, however, we require an additional vertex to be coarsened with  $V_6$  and independent from  $V_4$ . As  $V_6$  has no descendants, we must obtain this vertex from  $V_0, \dots, V_2$ , requiring an additional vertex to be conditioned on. For this reason, false-positive edges are especially likely to occur at the *end* of our chain.

## E.5 Test 3 Analysis

For  $p = 0.1$  to  $p = 0.3$  the medians of both true positive and true negative edge reconstruction are at 100%, with the distributions showing the occasional error. As the density of the graph increases, we fail to detect edges (lower blue marks), and incorrectly return edges where there are none (lower orange marks). At high densities, our accuracy for detecting true edges returns to higher levels, but at the cost of occasionally adding false positive edges. The second figure shows that these false positive edges may be due to the larger in-degree of more dense networks. We see very good recovery for networks with limited in-degree, and significantly more error with larger in-degrees.

## F Deferred Proofs

### F.1 Proof of Lemma 6

To prove this lemma we first define the entire set of descendants  $D_{ij} \supseteq \text{IMD}(V_i, V_j)$ .

**Definition 7.** Let the set  $D_{ij} := \text{DE}(V_i, V_j)$  be the descendants of both vertices and  $A_{ij} := V \setminus D_{ij}$ .

Recall that a separating set for any two sets of variables exists as a separating set in the moral graph of their ancestors (Lemma 12). By restricting our focus to  $\mathcal{S}_i, \mathcal{S}_j \subseteq \mathcal{A}_{ij}$  will also have  $\text{AN}^+(\mathcal{S}_i^+, \mathcal{S}_j^+) \subseteq \mathcal{A}_{ij}$  which guarantees that our separating sets will not overlap with  $\text{IMD}(V_i, V_j)$ . Lemma 18 will tell us how large we need  $\mathcal{A}_{ij}$  to be in order to be guaranteed an IPA.

**Lemma 18.** *An IPA  $\mathcal{S}_i^+, \mathcal{S}_j^+$  for  $V_i, V_j \in \mathcal{V}$  exists so long as  $|\mathcal{A}_{ij}| \geq (2 + \Delta^2)(\lceil \lg(k) \rceil + 1)$ .*

*Proof.* We can form  $\mathcal{S}_i^+$  out of  $V_i$  and  $\lceil \lg(k) \rceil$  arbitrary other vertices from  $\mathcal{A}_{ij}$ . Now, let the separating set be  $\mathcal{C} := \text{MB}^{\mathcal{G}[\mathcal{A}_{ij}]}(\mathcal{S}_i^+)$  and note that  $\mathcal{C}$  d-separates  $\mathcal{S}_i^+$  from all other elements of  $\mathcal{A}_{ij}$ . Since we know  $|\mathcal{C}| \leq \Delta^2(\lceil \lg(k) \rceil + 1)$ , we have at least  $\lceil \lg(k) \rceil$  vertices in  $\mathcal{A}_{ij}$  left to join with  $V_j$  and make  $\mathcal{S}_j^+$ .  $\square$

We are now ready to prove Lemma 6.

*Proof.* A convenient consequence of Lemma 18 is that it guarantees the existence of IPAs everywhere except within a small subset of vertices. Let  $\overline{\text{DE}}(V) := \mathcal{V} \setminus \text{DE}(V)$  be the “non-descendants” of  $V$ . Note that  $\mathcal{A}_{ij} = \overline{\text{DE}}(V_i) \cup \overline{\text{DE}}(V_j)$ . This implies that

$$|\mathcal{A}_{ij}| \geq \max(|\overline{\text{DE}}(V_i)|, |\overline{\text{DE}}(V_j)|). \quad (15)$$

Hence, so long as at least one vertex has enough non-descendants,  $\mathcal{A}_{ij}$  will be large enough to form an IPA. This set of vertices with enough non-descendants corresponds to the complement of the early vertices.  $\square$

## F.2 Proof of Lemma 2

*Proof.* We will drop the conditioning on  $\mathcal{c}$  in this proof for simplicity. Consider the sum

$$\sigma_j := \sum_{i=1}^j \Pr(u_i) \mathcal{M}[X, Y | u_i], \quad (16)$$

and note that  $\sigma_k = \mathcal{M}[X, Y]$ . Faithfulness with respect to  $\mathcal{G}'$  tells us that there is some assignment, which we call  $u_1$  wlog, such that  $X \not\perp\!\!\!\perp Y | u_1$ . Hence  $\text{rk}_+(\sigma_1) > 1$ .

Now, we show inductively that  $\text{rk}_+(\sigma_i) = \text{rk}_+(\sigma_{i-1}) + 1$  is a measure 1 event for  $i = 1, \dots, k$ . Denote  $\mathcal{M}[X, Y | u_i] = v_i w_i^\top$  with column space  $v_i$  drawn from a subspace with non-zero measure on  $\mathbb{R}^n$ . The column space of  $\sigma_{i-1}$  is rank  $\leq i-1 < m$ , so it has measure zero on  $\mathbb{R}^m$ . Hence,  $v_i$  being in the column space of  $\sigma_{i-1}$  is a measure 0 event. We conclude that  $\text{rk}_+(\sigma_{i-1} + \mathcal{M}^{u_i}[X, Y]) = \text{rk}_+(\sigma_{i-1}) + 1$  with measure 1. Inducting on  $i$  gives  $\text{rk}_+(\sigma_k) > k$  with measure 1.  $\square$

## F.3 Proof of Lemma 5

*Proof.* Suppose for contradiction that some vertex  $B \in \text{IMD}(V_i, V_j) \cap \mathcal{S}_j^+$ .  $B \in \text{IMD}(V_i, V_j)$  implies that there is a directed path  $\mathcal{P} \subseteq \text{IMD}(V_i, V_j)$  from  $V_i$  to  $B$ . By the definition of an IPA,  $B \in \mathcal{S}_j^+$  means that there must be some  $\mathcal{C}$  with  $B \perp\!\!\!\perp_d V_i | \mathcal{C}$ . We conclude that  $\mathcal{C}$  must contain some  $C \in \mathcal{P}$  in order to block  $\mathcal{P}$  from being an active path. However, this also means that  $C \in \text{IMD}(V_i, V_j)$ , which contradicts Observation 1. The same argument holds for  $B \in \mathcal{S}_i^+$ .  $\square$

## F.4 Proof of Lemma 8

*Proof.*  $\mathcal{T}_{ij}$  contains both  $\text{PA}(V_i)$  and  $\text{PA}(V_j)$ , so Lemma 10 tells us that we contain a separating set.  $\square$